11-2014

Structural Insights into the Architecture of the Hyperthermophilic Fusellovirus SSV1

Kenneth M. Stedman
Portland State University, kstedman@pdx.edu

Melissa DeYoung
Portland State University

Mitul Saha
University of Texas Medical Branch

Michael B. Sherman
University of Texas Medical Branch

Marc C. Morais
University of Texas Medical Branch

Citation Details

Kenneth M. Stedman, Melissa DeYoung, Mitul Saha, Michael B. Sherman, Marc C. Morais, Structural insights into the architecture of the hyperthermophilic Fusellovirus SSV1, Virology, Volume 474, 1 January 2015, Pages 105-109, ISSN 0042-6822, http://dx.doi.org/10.1016/j.virol.2014.10.014.

Virology 474 (2015) 105–109

Contents lists available at ScienceDirect

Virology

journal homepage: www.elsevier.com/locate/yviro

Brief Communication

Structural insights into the architecture of the hyperthermophilic *Fusellovirus* SSV1

Kenneth M. Stedman [a], Melissa DeYoung [a], Mitul Saha [b], Michael B. Sherman [b], Marc C. Morais [b,*]

[a] Center for Life in Extreme Environments, Biology Department, Portland State University, Portland, OR, USA
[b] Sealy Center for Structural Biology and Molecular Biophysics, Department of Biochemistry and Molecular Biology, University of Texas Medical Branch, Galveston, TX 77555, USA

ARTICLE INFO

Article history:
Received 2 June 2014
Returned to author for revisions
17 June 2014
Accepted 17 October 2014

Keywords:
SSV
SSV1
Fusellovirus
Fullerene cone
Virus assembly
Virus structure
Archaeal virus
Extremophile
Hyperthermophilic virus
Spindle-shaped virus

ABSTRACT

The structure and assembly of many icosahedral and helical viruses are well-characterized. However, the molecular basis for the unique spindle-shaped morphology of many viruses that infect *Archaea* remains unknown. To understand the architecture and assembly of these viruses, the spindle-shaped virus SSV1 was examined using cryo-EM, providing the first 3D-structure of a spindle-shaped virus as well as insight into SSV1 biology, assembly and evolution. Furthermore, a geometric framework underlying the distinct spindle-shaped structure is proposed.

Introduction

The morphological diversity of viruses that infect hyperthermophilic *Archaea* vastly exceeds that of other known prokaryotic viruses (Prangishvili, 2003; Prangishvili et al., 2006). Indeed, unique features of these viruses have necessitated the introduction of 10 novel virus families: e.g. filamentous *Lipothrixviridae*, rod-shaped *Rudiviridae*, droplet-shaped *Guttaviridae*, and spindle-shaped *Fuselloviridae*. There are also numerous unclassified archaeal spindle-shaped viruses (Prangishvili, 2013). This diversity may reflect ancestral diversity of viral morphotypes present in hot environments during the prebiotic phase of evolution (Balter, 2000; Prangishvili, 2003; Prangishvili et al., 2006). Furthermore, because hyperthermophilic *Archaea* possess metabolisms well-suited for primordial hot anaerobic conditions, it has also been suggested that hyperthermophilic viruses may have played an important role at the earliest stages of evolution (Prangishvili, 2003).

Despite the unusual morphologies of archaeal viruses, studies on their genome organization, mechanism of replication, and regulation of gene expression indicate a distant evolutionary relationship between some of these viruses and viruses of mesophilic bacteria and eukaryotes (Blum et al., 2001; Iyer et al., 2006; Klein et al., 2002; Peng et al., 2001; Pfister et al., 1998; Prangishvili, 2003; Tang et al., 2004; Tang et al., 2002). Verification of this hypothesis by sequence comparison is challenging because the rapid evolution of viral genes can preclude detection of relationships over large evolutionary distances (Pagel, 1999). However, structural similarity often persists during evolution in spite of vanishing sequence similarity. For example, capsid proteins adopting either the jelly-roll or HK97 fold have been observed in icosahedral viruses infecting each of the three domains of life, suggesting that the ancestors of viruses utilizing these capsid protein folds predates the last universal common (cellular) ancestor (LUCA) (Fokine et al., 2004; Jiang et al., 2003; Khayat and Johnson, 2011; Morais et al., 2005; Pietila et al., 2013; Wikoff et al., 2000). Thus, the structural information regarding the morphologically divergent viruses infecting hyperthermophilic *Archaea* might provide insights into virus origin and the evolution of viruses and cells. Here, cryo-EM image analysis and reconstruction

* Corresponding author.
E-mail address: mcmorais@utmb.edu (M.C. Morais).

http://dx.doi.org/10.1016/j.virol.2014.10.014
0042-6822/

was used to structurally characterize the prototypical Sulfolobus fusellovirus SSV1 (Contursi et al., 2014), providing insight into the underlying geometry and assembly of the spindle-shaped capsid. In addition to a ~15 kbp positively supercoiled dsDNA genome, purified SSV1 virions are composed of; a major capsid protein, VP1; a minor capsid protein with very similar sequence, VP3; a DNA binding protein, VP2; and smaller amounts of the products of ORFs C792 and D244 (Menon et al., 2008; Reiter et al., 1987).

Results and discussion

Although no symmetry was initially assumed, preliminary cycles of the iterative refinement procedure indicated that D1 symmetry (two-fold symmetry perpendicular to the long-axis of the virus) could be applied to the virus capsid and six-fold symmetry applied to the tail. Upon convergence of refinement, the resolution of the reconstruction was ~32 Å as estimated using a Fourier shell correlation cutoff of 0.5 between independent half-data sets. Resolution was likely limited by particle size, lack of global symmetry, structural heterogeneity, and the relatively small number of particles included in the reconstruction, although ~doubling the number of particles did not result in any measurable improvement in the map. At the current resolution, there is no indication of an internal or external membrane despite that SSVs are apparently released by budding and have a low buoyant density (1.27 g/mL) (Martin et al., 1984). Moreover density for the packaged DNA is more diffuse than is observed for dsDNA bacteriophages, possibly due to the relatively small size (~15 kbp) of the SSV1 genome and/or its unusual positively supercoiled topology (Nadal et al., 1986; Palm et al., 1991). The SSV1 reconstruction (Fig. 1B–D) indicated that the capsid is ~750 Å long, and ~430 Å wide at the equator, and that the tail is ~120 Å long by 120 Å wide. The long dimension is consistent with TEM analysis of negatively stained SSV1 virions at ~1000 Å, however the narrow dimension, reported as 600 Å less so (Martin et al., 1984); the wider dimensions observed in negative stain are likely due to flattening of the particles during grid preparation, a common

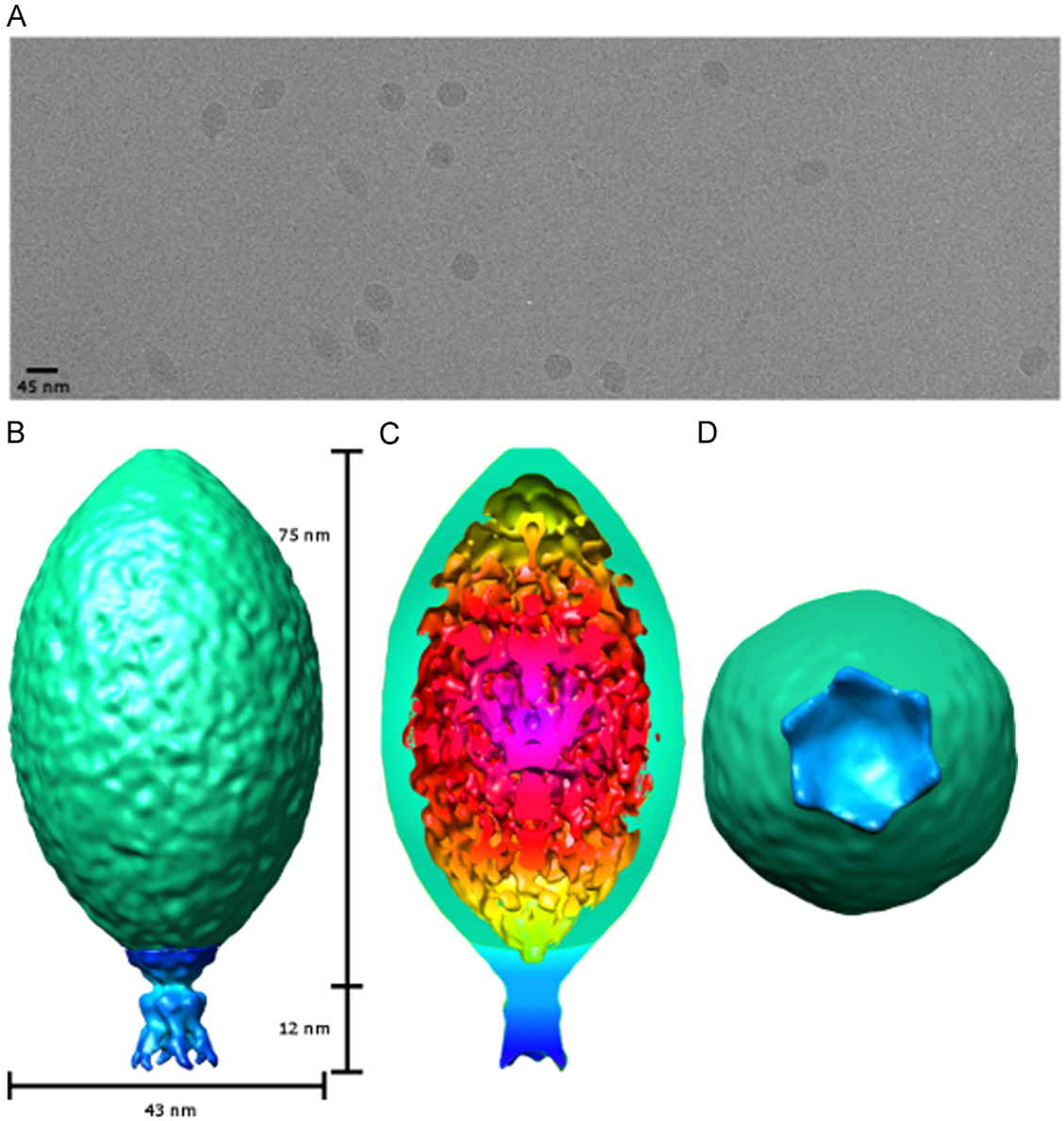

Fig. 1. Cryo-EM analysis of SSV1 particles. A) Typical field of particles. Three-dimensional reconstruction of an SSV1 particle from a side-view (A), side-view cross-section (B), and end-on view looking at the tail (C). In all panels, the capsid is colored green, and the approximate density corresponding to the is colored tail blue; in panel (C), density within the capsid, presumably corresponding to the viral genome, is colored from magenta to yellow according to radial distance from the center of the particle.

occurrence in negative-stained images of viral particles. The diameter of the hexameric tail is similar to the size of hexameric and trimeric pores observed in the P3 S-layer glycoprotein lattice on the surface of the archaeal *Sulfolobus* host (Deatherage et al., 1983; Veith et al., 2009); this complementarity of size and shape may facilitate host recognition and attachment by the virus. Furthermore, mutually induced conformational changes in the tail and the S-layer upon virus–host binding could provide a means of initiating infection.

The six-fold symmetric tail is reminiscent of dsDNA bacteriophage, where the six-fold symmetry axis of the tail is coincident with a five-fold symmetry axis of the icosahedral capsid. However, imposition of five-fold symmetry to the SSV1 capsid did not result in noticeable improvement to the reconstruction, and instead resulted in a smooth featureless capsid such as would be expected from inappropriate symmetry averaging. Thus, unlike the dsDNA bacteriophages, the geometry of SSV1 capsids is likely not derived from simple isometric or prolate icosahedral symmetry. However, regular arrays of capsomers arranged on an approximately hexagonal lattice are apparent when the map is viewed at high contour levels (Fig. 2). The approximate spacing between capsomers is ~50 Å (Fig. 2), considerably smaller than spacing between capsomers constructed from either a jelly roll fold (~70 Å) or the HK97 fold (~140 Å) (Fokine et al., 2004; Khayat and Johnson, 2011; Morais et al., 2005). Hence it is unlikely that the SSV1 capsid protein adopts either of these ubiquitous viral capsid folds, consistent with lack of sequence similarity between SSV1 major capsid protein vp1 and any other viral capsid proteins (Prangishvili, 2003; Prangishvili et al., 2006). However, due to the low resolution of the map, we cannot rule out the possibility that the protein assumes one of these folds, but is arranged differently on the capsid lattice.

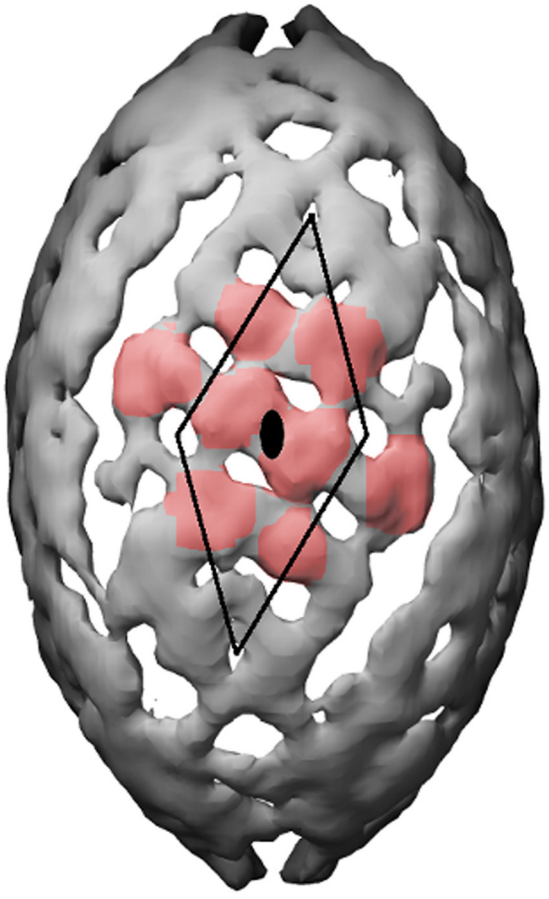

Fig. 2. Reconstruction of an SSV1 particle viewed at high contour level. Seven potential capsomers arranged in an approximately hexagonal lattice are colored orange, and one pseudo P6 unit cell is shown as a black rhomboid.

To form a closed three-dimensional volume from a hexagonal array of identical subunits, 12 hexamers must be replaced with pentamers. In isometric and prolate icosahedrons, there are 6 pentamers at either end of the object. Clearly, the elongated shape of SSV1 is incompatible with isometric icosahedral symmetry. Similarly, the lack of 5-fold symmetry along the long axis of the virus and the absence of a cylindrical equatorial region rule out prolate icosahedral symmetry as well. One possible explanation for the observed morphology of SSV1, and spindle-shaped viruses in general, is that their capsid resembles two fused fullerene cones (Fig. 3). In these cones, there are different numbers of pentamers at either end of the cone, resulting in their distinct asymmetric cone-shape; for example, the well-characterized HIV cone has five pentamers at its narrow end and 7 pentamers at its wide end (Benjamin et al., 2005; Ganser et al., 1999; Pornillos et al., 2009). The ~60° angles of narrow ends of the SSV1 reconstruction are consistent with two "fused" $P=3$ fullerene cones (Fig. 3A and B). A single $P=3$ cone would have 3 pentamers at its conical tip. A structure consisting of two "fused" cones, such as is proposed here for SSV1 particles, would thus have three pentamers at either end, and six additional pentamers distributed across its equatorial region. Although the structure shown in Fig. 3 has D3 point group symmetry, other structures, with different positions of the 12 pentamers, can also be formed via fusion of two $P=3$ fullerene cones. It may be that the observed heterogeneity of particles arises, at least in part, from pentamers being incorporated at different positions in individual particles. Furthermore morphological variation among spindle-shaped virus, both within and between different species, may result from different numbers of pentamers at the spindle ends and equatorial regions, which would result in different cone angles, as well as from different cone lengths resulting from incorporation of more/fewer hexamers between the cone ends and the equatorial region. Regardless, it seems unlikely that spindle-shaped capsids actually assemble via the fusion of two separate cones, but rather nucleate from a specific site, possibly the tail vertex, to assemble the observed structure. Confirmation of this model awaits higher resolution structural information regarding spindle-shaped viruses.

Materials and methods

SSV1 growth and purification has been previously described (Stedman et al., 2010; Schleper et al., 1992). Briefly, virus was purified from infected *Sulfolobus solfataricus* strain PH1 (Schleper et al., 1994) and particles isolated from culture supernatants by centrifugation and filtration. The viral titer was ~10^5 PFU/mL as determined by semi-quantitative spot-on-lawn assays (Stedman et al., 2003). The virions were concentrated to ~10^{11} particles/ml using ultra-filtration (Stedman et al., 2010). Approximately 4 μl of purified SSV1 particles were flash-frozen on holey carbon grids in liquid ethane. Images were initially recorded on film with an approximate electron dose of 20 $e^-/Å^2$, a defocus range of ~1.2–3.1 μm, and at 33,000× magnification on a CM300 FEG microscope. Micrographs were digitized at 4.24 Å pixel − 1 with a Zeiss SCAI scanner. 932 Individual particles from 34 images were boxed, floated, and preprocessed to normalize mean intensities and variances and to remove linear background gradients. Structure factor phases and amplitudes were modified as indicated by the parameters of the contrast transfer function. Initial classification of the data by reference free alignment (Frank, 2002) indicated that predominantly side views of the particles were present and that the population was somewhat morphologically heterogeneous

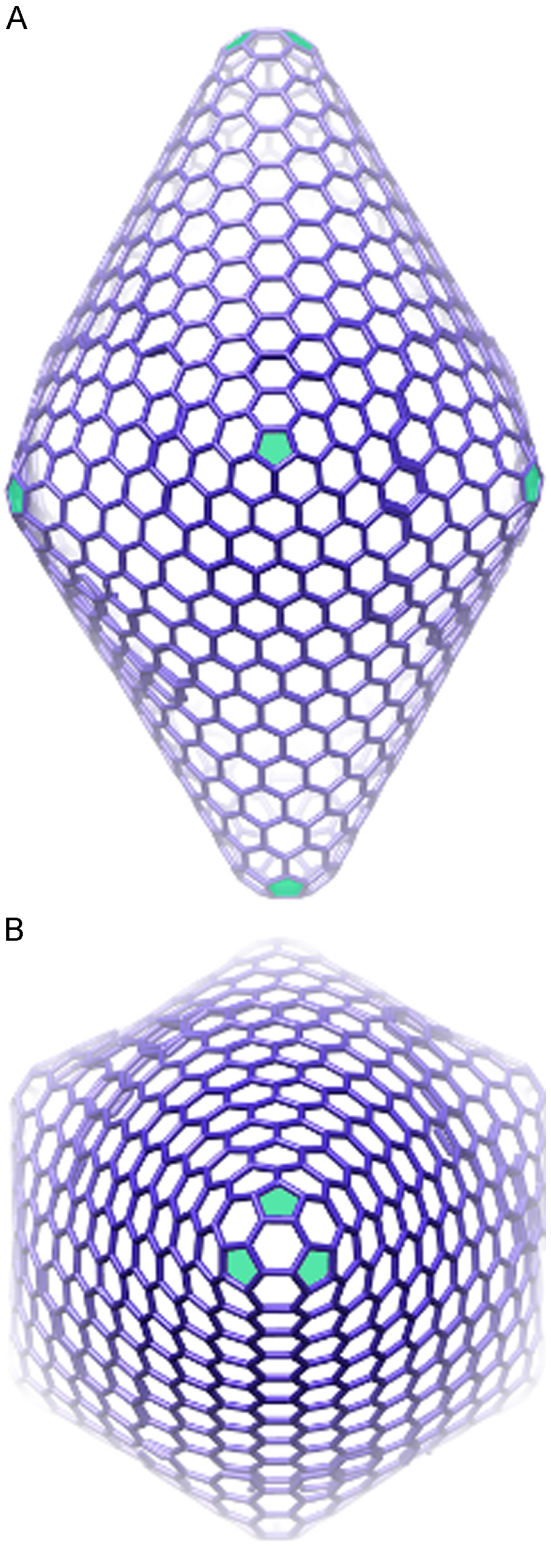

Fig. 3. One potential structure resulting from fusion of two $P=3$ fullerene cones is shown, with pentamers colored green, from a side (A) and end-on (B) view. This particular structure has D3 point group symmetry, with three pentamers at either end and an additional six distributed around the equatorial region. Other structures, with different positions of pentamers, can also be formed via fusion of two $P=3$ fullerene cones.

(Fig. 1A). The heterogeneous morphology of SSV1 virions has been known since its discovery (Martin et al., 1984). Although most of the particles were of similar size and shape, there were also many particles that were clearly larger or deformed in some obvious way; such particles were identified by eye and excluded from further analysis and image reconstruction. An initial model of an SSV1 particle corresponding to the most common morphology was generated as follows: 1) a single class-average of a side view was rotated such that the long axis of the virus was aligned with a projection of the *Z*-axis of the image-processing coordinate system; 2) five copies of the rotated image were each assigned orientations that differed only by multiples of $2\pi/5$ rad (72°) around the *Z*-axis; 3) these five images were then used to reconstruct a 3D-volume using Fourier–Bessel methods (Crowther et al., 1970) This volume was used as a starting point for alignment of additional particles via model-based projection matching. All image processing steps were performed using EMAN (Ludtke et al., 1999).

Funding

This work was supported by Portland State University and National Science Foundation Research Grant 1243963 (to K.M.S. and M.C.M.) and Grant 0702020 to K.M.S.

Acknowledgments

We would like to acknowledge the Sealy Center for Structural and Molecular Biophysics for support of the UTMB cryo-EM core facility.

References

Balter, M., 2000. Virology. Evolution on life's fringes. Science 289, 1866–1867.
Benjamin, J., Ganser-Pornillos, B.K., Tivol, W.F., Sundquist, W.I., Jensen, G.J., 2005. Three-dimensional structure of HIV-1 virus-like particles by electron cryotomography. J. Mol. Biol. 346, 577–588.
Blum, H., Zillig, W., Mallok, S., Domdey, H., Prangishvili, D., 2001. The genome of the archaeal virus SIRV1 has features in common with genomes of eukaryal viruses. Virology 281, 6–9.
Contursi, P., Fusco, S., Canniio, R., She, Q., 2014. Molecular biology of fuselloviruses and their satellites. Extremophiles 18, 473–489.
Crowther, R.A., Amos, L.A., Finch, J.T., De Rosier, D.J., Klug, A., 1970. Three dimensional reconstructions of spherical viruses by fourier synthesis from electron micrographs. Nature 226, 421–425.
Deatherage, J.F., Taylor, K.A., Amos, L.A., 1983. Three-dimensional arrangement of the cell wall protein of *Sulfolobus acidocaldarius*. J. Mol. Biol. 167, 823–848.
Fokine, A., Chipman, P.R., Leiman, P.G., Mesyanzhinov, V.V., Rao, V.B., Rossmann, M.G., 2004. Molecular architecture of the prolate head of bacteriophage T4. Proc. Natl. Acad. Sci. USA 101, 6003–6008.
Frank, J., 2002. Single-particle imaging of macromolecules by cryo-electron microscopy. Annu. Rev. Biophys. Biomol. Struct. 31, 303–319.
Ganser, B.K., Li, S., Klishko, V.Y., Finch, J.T., Sundquist, W.I., 1999. Assembly and analysis of conical models for the HIV-1 core. Science 283, 80–83.
Iyer, L.M., Balaji, S., Koonin, E.V., Aravind, L., 2006. Evolutionary genomics of nucleocytoplasmic large DNA viruses. Virus Res. 117, 156–184.
Jiang, W., Li, Z., Zhang, Z., Baker, M.L., Prevelige Jr., P.E., Chiu, W., 2003. Coat protein fold and maturation transition of bacteriophage P22 seen at subnanometer resolutions. Nat. Struct. Biol. 10, 131–135.
Khayat, R., Johnson, J.E., 2011. Pass the jelly rolls. Structure 19, 904–906.
Klein, R., Baranyi, U., Rossler, N., Greineder, B., Scholz, H., Witte, A., 2002. Natrialba magadii virus phiCh1: first complete nucleotide sequence and functional organization of a virus infecting a haloalkaliphilic archaeon. Mol. Microbiol. 45, 851–863.
Ludtke, S.J., Baldwin, P.R., Chiu, W., 1999. EMAN: semiautomated software for high-resolution single-particle reconstructions. J. Struct. Biol. 128, 82–97.
Martin, A., Yeats, S., Janekovic, D., Reiter, W.D., Aicher, W., Zillig, W., 1984. SAV 1, a temperate u.v.-inducible DNA virus-like particle from the archaebacterium *Sulfolobus acidocaldarius* isolate B12. EMBO J. 3, 2165–2168.
Menon, S.K., Maaty, W.S., Corn, G.J., Kwok, S.C., Eilers, B.J., Kraft, P., Gillitzer, E., Young, M.J., Bothner, B., Lawrence, C.M., 2008. Cysteine usage in *Sulfolobus* spindle-shaped virus 1 and extension to hyperthermophilic viruses in general. Virology 376, 270–278.
Morais, M.C., Choi, K.H., Koti, J.S., Chipman, P.R., Anderson, D.L., Rossmann, M.G., 2005. Conservation of the capsid structure in tailed dsDNA bacteriophages: the pseudoatomic structure of phi29. Mol. Cell 18, 149–159.
Nadal, M., Mirambeau, G., Forterre, P., Reiter, W.-D., Duguet, M., 1986. Positively supercoiled DNA in a virus-like particle of an archaebacterium. Nature 321, 256–258.

Pagel, M., 1999. Inferring the historical patterns of biological evolution. Nature 401, 877–884.
Palm, P., Schleper, C., Grampp, B., Yeats, S., McWilliam, P., Reiter, W.D., Zillig, W., 1991. Complete nucleotide sequence of the virus SSV1 of the archaebacterium *Sulfolobus shibatae*. Virology 185, 242–250.
Peng, X., Blum, H., She, Q., Mallok, S., Brugger, K., Garrett, R.A., Zillig, W., Prangishvili, D., 2001. Sequences and replication of genomes of the archaeal rudiviruses SIRV1 and SIRV2: relationships to the archaeal lipothrixvirus SIFV and some eukaryal viruses. Virology 291, 226–234.
Pfister, P., Wasserfallen, A., Stettler, R., Leisinger, T., 1998. Molecular analysis of *Methanobacterium* phage psiM2. Mol. Microbiol. 30, 233–244.
Pietila, M.K., Laurinmaki, P., Russell, D.A., Ko, C.C., Jacobs-Sera, D., Hendrix, R.W., Bamford, D.H., Butcher, S.J., 2013. Structure of the archaeal head-tailed virus HSTV-1 completes the HK97 fold story. Proc. Natl. Acad. Sci. USA 110, 10604–10609.
Pornillos, O., Ganser-Pornillos, B.K., Kelly, B.N., Hua, Y., Whitby, F.G., Stout, C.D., Sundquist, W.I., Hill, C.P., Yeager, M., 2009. X-ray structures of the hexameric building block of the HIV capsid. Cell 137, 1282–1292.
Prangishvili, D., 2003. Evolutionary insights from studies on viruses of hyperthermophilic archaea. Res. Microbiol. 154, 289–294.
Prangishvili, D., 2013. The wonderful world of archaeal viruses. Annu. Rev. Microbiol. 67, 565–585.
Prangishvili, D., Forterre, P., Garrett, R.A., 2006. Viruses of the Archaea: a unifying view. Nat. Rev. Microbiol. 4, 837–848.
Reiter, W.D., Palm, P., Yeats, S., Zillig, W., 1987. Gene expression in archaebacteria: physical mapping of constitutive and UV-inducible transcripts from the *Sulfolobus* virus-like particle SSV1. Mol. Gen. Genet. 209, 270–275.
Schleper, C., Kubo, K., Zillig, W., 1992. The particle SSV1 from the extremely thermophilic archaeon *Sulfolobus* is a virus: demonstration of infectivity and of transfection with viral DNA. Proc. Natl. Acad. Sci. USA 89, 7645–7649.
Schleper, C., Roder, R., Singer, T., Zillig, W., 1994. An insertion element of the extremely thermophilic archaeon *Sulfolobus solfataricus* transposes into the endogenous beta-galactosidase gene. Mol. Gen. Genet. 243, 91–96.
Stedman, K.M., She, Q., Phan, H., Arnold, H.P., Holz, I., Garrett, R.A., Zillig, W., 2003. Relationships between fuselloviruses infecting the extremely thermophilic archaeon *Sulfolobus*: SSV1 and SSV2. Res. Microbiol. 154, 295–302.
Stedman, K.M., Porter, K., Dyall-Smith, M., 2010. The isolation of viruses infecting Archaea. In: Wilhelm, S.W., Weinbauer, M.G., Suttle, C.A. (Eds.), Manual of Aquatic Viral Ecology. American Society of Limnology and Oceanography, Waco, TX, pp. 57–64.
Tang, S.L., Nuttall, S., Dyall-Smith, M., 2004. Haloviruses HF1 and HF2: evidence for a recent and large recombination event. J. Bacteriol. 186, 2810–2817.
Tang, S.L., Nuttall, S., Ngui, K., Fisher, C., Lopez, P., Dyall-Smith, M., 2002. HF2: a double-stranded DNA tailed haloarchaeal virus with a mosaic genome. Mol. Microbiol. 44, 283–296.
Veith, A., Klingl, A., Zolghadr, B., Lauber, K., Mentele, R., Lottspeich, F., Rachel, R., Albers, S.V., Kletzin, A., 2009. *Acidianus*, *Sulfolobus* and *Metallosphaera* surface layers: structure, composition and gene expression. Mol. Microbiol. 73, 58–72.
Wikoff, W.R., Liljas, L., Duda, R.L., Tsuruta, H., Hendrix, R.W., Johnson, J.E., 2000. Topologically linked protein rings in the bacteriophage HK97 capsid. Science 289, 2129–2133.